APPENDIX

Publications

ScieTech 2013 IOP Publishing
Journal of Physics: Conference Series **423** (2013) 012042 doi:10.1088/1742-6596/423/1/012042

Wettability Effect of PECVD-SiO_x Films on Poly(lactic acid) Induced by Oxygen Plasma on Protein Adsorption and Cell Attachment

S Sarapirom[1], J S Lee[2], S B Jin[2], D H Song[3], L D Yu[1,4], J G Han[2] and C Chaiwong[1,4]

[1] Plasma and Beam Physics Research Facility, Department of Physics and Materials Science, Faculty of Science, Chiang Mai University, Chiang Mai 50200, Thailand
[2] Institute for Plasma-Nano Materials, Center of Advanced Plasma Surface Technology, Sungkyunkwan University, 300 ChunChun-dong, Jangan-gu, Suwon 440-746, Korea
[3] Department and Research Institute of Dental Biomaterials and Bioengineering, College of Dentistry, Yonsei University, 250 Seongsanno, Seodaemun-gu, Seoul 120-752, Korea
[4] Thailand Center of Excellence in Physics, Commission on Higher Education, 328 Si Ayutthaya Rd., Bangkok 10400, Thailand

E-mail: cchwng@gmail.com

Abstract. Surface wettability is an important property of biomaterials. Silicon oxide films have a wide range of applications due to a range of the properties such as the mechanical strength and surface wettability. This paper reports effect of the surface wettability of silicon oxide (SiO_x) films on protein adsorption and cell attachment and proliferation. SiO_x films were deposited onto poly(lactic acid) (PLA) substrate using plasma enhanced chemical vapor deposition (PECVD). Octamethylcyclotetrasiloxane (OMCTS:$Si_4O_4C_8H_{24}$) was used as a precursor with O_2 as a carrier gas. After deposition, the films were treated with O_2-plasma to adapt wettability. It was found that O_2-plasma enhanced the wettability of the films without changing the film thickness, while made the surface morphology slightly smoother. The polar component increased after O_2-plasma treatment as observed in the contact angle measurements. The surface energy of the films was calculated by means of the Owens-Wendt method to resolve the contributions of polar and dispersive components. The chemical structure was characterized using attenuated total reflectance-Fourier transform infrared (ATR-FTIR) spectroscopy. The films were dense with a high Si-network structure. The reduced carbon content (-CH_n, Si-CH_3) and increased hydrogen content (-OH) of the O_2-plasma treated SiO_x films led to the polar components enhancing the SiO_x wettability. Adsorption of bovine serum albumin (BSA) on the films was investigated by using x-ray photoelectron spectroscopy (XPS). More BSA was adsorbed onto the O_2-plasma treated SiO_x films. Attachment and proliferation of MC3T3-E1 mouse pre-osteoblasts and L929 mouse fibroblasts cells on the SiO_x films were evaluated via MTT assay. The cells were attached more to the untreated SiO_x films but proliferated more on the surface of the O_2-plasma treated SiO_x films depending on the cell types.

1. Introduction

Biomaterials have been important in transplantation medicine, tissue engineering, and bioartificial tissues. For advanced applications, they should not only be biocompatible but also specifically

designed for peculiar cellular response, such as cell attachment, proliferation, and differentiation. Common interaction between material and biological systems occurs in a wide range of applications. While biomaterial is in contact with a biological environment, protein adsorption first takes place before other processes such as platelet or blood cell adhesion, and then cells contact with a protein layer on the material surface. Consequently, protein-surface interaction is critical to understanding for control and design of biomaterials.

There are several methods to modify the surfaces properties of biomaterials [1, 2], and each way depends on the objectives. For example, adhesive proteins (fibronectin, vitronectin or collagen) are immobilized onto different wettability surface for improving cells attachment or promoting specific interaction for biosensor/microarray [3-5], and bovine serum albumin is immobilized on hydrophobic and hydrophilic surface for blocking of non-pacific proteins [6]. Moreover, thin film coating on the materials can lead to excellent mechanical properties and biocompatibility of biomaterials. For instance, titanium dioxide improved cells-surface interaction [7], and silicon oxide films promoted selective adhesion of protein or cells to materials [8, 9].

Thin films of silicon-organic compounds are used in a range of applications. The characteristics of the films can be tailored by changing deposition process parameters. Polymer-like films are applied in optoelectronic devices, and protective coatings for different substrates. Quartz-like films can be used as diffusion barriers [10, 11]. In recent years, there is a growing interest in developing silicon oxide films for use in biomedical applications such as bioelectronics, and biofunctional materials. Plasma enhanced chemical vapor deposition (PECVD) is widely used to deposit silicon oxide films on polymeric biomaterials [12] because it can adjust the mechanical properties with the deposition parameters. Oxygen (O_2) plasma was used to adapt wettability of SiO_x films because O_2 plasma enhanced higher O_2-containing functionalities and more drastic morphology change leading to proteins and cells attachment [13, 14].

The adsorption of proteins in the blood plasma on the biomaterial surface is, in general, a dynamic phenomenon since there is a competition in the adsorption process of such proteins. Albumin (Alb) is the most abundant protein in blood plasma and able to bind with other molecules. It is usually employed as a model protein to be studied in protein-surface interactions. In an aqueous environment, proteins will tend to adopt both a hydrophobic and a hydrophilic surface. Proteins can be irreversibly bound to a hydrophobic surface through the dehydration of the interface and undergoes conformation changes. According to the Vroman effect, low-molecular-weight protein such as Alb is first adsorbed on the surface then higher molecular weight proteins, such as fibronectin [15]. Thus, if Alb is adsorbed with irreversible bonds, the cell adhesion protein can follow and enhance cell attachment and proliferation.

In this work, we were interested in and thus studied effect of wettability of silicon oxide films on protein adsorption, cell attachment and proliferation. Post-deposition O_2-plasma treatment was applied to modify the surface wettability of SiO_x films which were deposited on polymer using PECVD. The research results would be beneficial to certain biomedicine application potentials such as polymeric cell-culture dishes and biosensors whose cell attachment and proliferation properties could be modified by depositing SiO_x thin films.

2. Experiment

2.1. Materials preparation and modification

Poly(lactic acid) (PLA) membranes of (thickness 50 μm), obtained from the School of Mechanical Engineering, Institute of Engineering, Suranaree University of Technology, Thailand were used as the substrate. The membranes were cut into 1 cm × 4 cm strips.

SiO_x films were deposited on the PLA membranes by PECVD in Sungkyunkwan University, Korea using octamethylcyclotetrasiloxane (OMCTS: $Si_4O_4C_8H_{24}$) with oxygen as a carrier gas. The details of the deposition has been described elsewhere [12]. In brief, the membrane substrate samples were put on a glass slide sample holder in the PECVD chamber and the chamber was evacuated to a base

pressure of 0.01 Pa. To remove the residues and increase films adhesion, the membranes were first sputtered using O_2-plasma at 3.3 Pa by a bottom electrode with a radio frequency (RF) power of 60 W for 20 seconds. After that, SiO_x films were deposited at an OMCTS vapor pressure of 3.3 Pa by a top electrode with an RF power of 120 W and a bottom electrode with an RF power of 60 W for 40 seconds. Then, for increasing the hydrophilicity, a part of the SiO_x films were further treated using O_2-plasma at 3.3 Pa and a bottom electrode with an RF power of 60 W for 60 seconds.

2.2. Surface characterization

The thickness of the deposited film was measured using an Alpha-Step IQ Surface Profiler (KLA-Tencor, USA). The film surface morphology was observed using atomic force microscopy (AFM) (Thermo Microscope Autoprobe CP-Research, USA). The AFM images were acquired in the contact mode using silicon tips with a scan rate of 1 Hz in air. The images were analyzed to measure the root mean square (Rms) and the surface-peak-to-valley roughness (Rp-v).

The static contact angles were measured with 2 µl of deionized water and diiodomethane (CH_2I_2), respectively, at room temperature. The image of the fluid drops was captured and analyzed by using the image analysis software. The surface energy was calculated using the Owens-Wendt equations [16, 17], which are expressed as follows:

$$\gamma_W(1+\cos\theta_W) = 2\sqrt{\gamma_S^d\gamma_W^d} + 2\sqrt{\gamma_S^p\gamma_W^p} \quad (1)$$

$$\gamma_D(1+\cos\theta_D) = 2\sqrt{\gamma_S^d\gamma_D^d} + 2\sqrt{\gamma_S^p\gamma_D^p} \quad (2)$$

where γ is the surface energy, θ is the contact angle, and the superscripts, d and p, represent the dispersive component and the polar component of the surface energy, respectively. The Subscript S, D, and W indicate solid, diiodomethane and water, erspectively. For water, γ_W = 72.8 mJ/m^2, γ_W^d = 22.1 mJ/m^2, and γ_W^p = 50.7 mJ/m^2. For diiodomethane, γ_D = 50.8 mJ/m^2, γ_D^p = 44.1 mJ/m^2, and γ_D^d = 6.7 mJ/m^2 [18].

The chemical structure of the film was characterized using attenuated total reflectance-Fourier transform infrared (ATR-FTIR) spectroscopy (Bruker-Optics) with germanium crystal. Each spectrum was obtained using an average of 64 scans in the range of 400-4000 cm^{-1} with a resolution of 4 cm^{-1}.

2.3. Protein adsorption analysis

The bovine serum albumin (BSA)(A2153) was purchased from Sigma-Aldrich Corporation, Germany. Strips of the films were cut into 1 cm × 1 cm and placed into wells of a 4-well plate. The protein was immobilized onto the films by adding 1 ml of BSA solution (0.5% W/V in distilled water) into each well and then incubated for 20 min on a rocking shaker at room temperature. After incubation, the films were washed in distilled water for 20 min, first soaking and then rinsing 3 times. The films were dried in a new plate and left at room temperature for 12 h. Some films were analyzed for the chemical structure using x-ray photoelectron spectroscopy (XPS) (Shimadzu, Japan) [19, 20]. Survey spectra of XPS were acquired from 0-1200 eV, with a pass energy of 80 eV and step size of 1 eV. The core level spectra (high-resolution spectra) were obtained with a pass energy of 20 eV and step size of 0.1 eV. Elemental compositions were calculated from peak areas obtained from the survey spectra. All XPS peaks were referenced to a C_{1s} signal at a binding energy of 284.6 eV, corresponding to the C-C and C-H bonds in hydrocarbons. The peaks were deconvoluted into Gaussian components to gain the insight into the bonding.

2.4. Cell culture

Fibroblast cells are normally used as a model of cell attachment and proliferation since they are the most common cells of connective tissues in animals and able to grow in a high rate. In this investigation, mouse fibroblast cells (L929) and mouse pre-osteoblast cells (MC3T3-E1) were used to study cell cultivation on the surfaces of the as-deposited SiO_x and O_2-plasma treated SiO_x films. Use

of the fibroblast cells was aimed at artificial tissue test and use of the osteoblast cells was aimed at scaffold test. The cell attachment and proliferation were evaluated using MTT assay. The films were first sterilized under ultraviolet (UV) light for 1 h (both faces). The cells were diluted to 5×10^3 cells/ml. The culture medium was modified with 10% fetal bovine serum and 1% antibiotic antimycotic solution (WelGENE, Korea). The cells were cultured at 37°C in a 5%-humidified CO_2-atmosphere incubator. Then cell seeding films were measured with a fluorescence spectrometer at wavelengths of 544 and 590 nm. In these experiments, 3 replicates were used for calculating the percentage of each experiment. The cell attachment was observed in 1 day and cell proliferations were observed in 3 and 7 days.

3. Results and discussion

3.1. Surface characterization

The thickness of the as-deposited SiO_x films was 48.2±0.5 nm and that of the O_2-plasma treated SiO_x films was 47.8±0.8 nm as measured by the surface profiler. The film thickness was decreased by O_2-plasma treatment insignificantly, indicating that the O_2-plasma treatment did not have noticeable effect on changing the thickness of SiO_x films. Surface morphology of the films was observed by AFM with a scanning area of 3μm × 3μm. Roughness data were obtained from different regions on each sample. Figure1 shows the AFM images of the as-deposited SiO_x film and the O_2-plasma treated SiO_x film. The O_2-plasma treatment decreased the surface roughness (root-mean-square, R_{rms}) of the films from 26 nm to 19 nm due to plasma etching effect.

The material surface energy consists of polar and non-polar components. The polar component of surface energy comprises all other interactions due to the non-London forces. Polar molecules interact with dipole forces and hydrogen bonds. The dispersive or non-polar components of surface energy result from molecular interactions due to the London forces [21]. Figure 2a shows the results of the contact angle measurements. The water contact angle of the as-deposited SiO_x films was 57.0 degree and after O_2-plasma treatment the water contact angle obtained was significantly decreased down to 2.7 degrees, showing a significant increase in the hydrophilicity of the film. Figure 2b shows the components of the surface energy of the films. The polar components of the surface energy increased after O_2-plasma treatment. The total surface energy was higher after the O_2-plasma treatments, demonstrating that the surface of SiO_x became more hydrophilic. The enhanced hydrophilicity of the O_2-plasma treated SiO_x films was owing to increased polarity, as there were more polar components in the total surface energy. This could result from the incorporation of polar groups such as hydroxyl group on the surface.

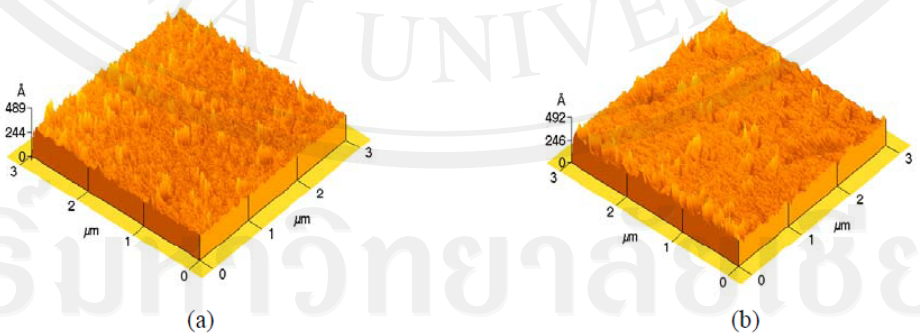

Figure 1. AFM images of the surface morphology of (a) as-deposited SiO_x and (b) O_2-plasma treated SiO_x films.

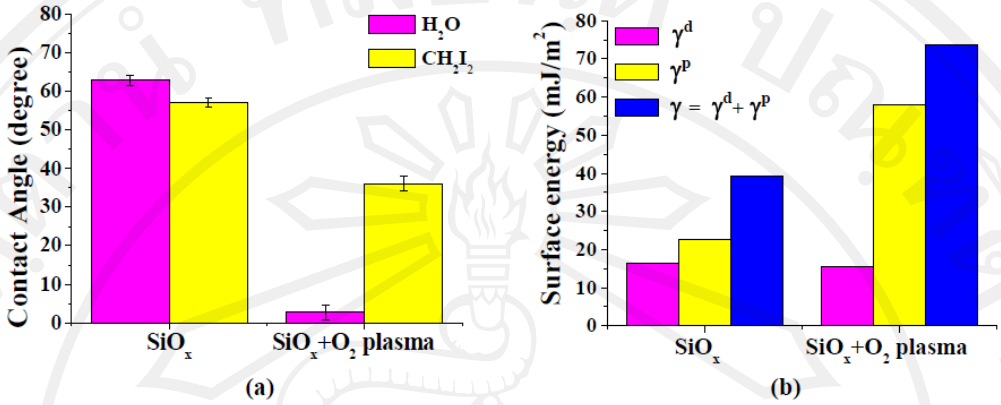

Figure 2. Surface properties of the SiO_x films. (a) Contact angle of water (H_2O) and diiodomethane (CH_2I_2) on the as-deposited SiO_x film and O_2-plasma treated SiO_x film. (b) Surface energy of the as-deposited SiO_x film and O_2-plasma treated SiO_x film, including dispersive components : γ_S^d and polar components : γ_S^p.

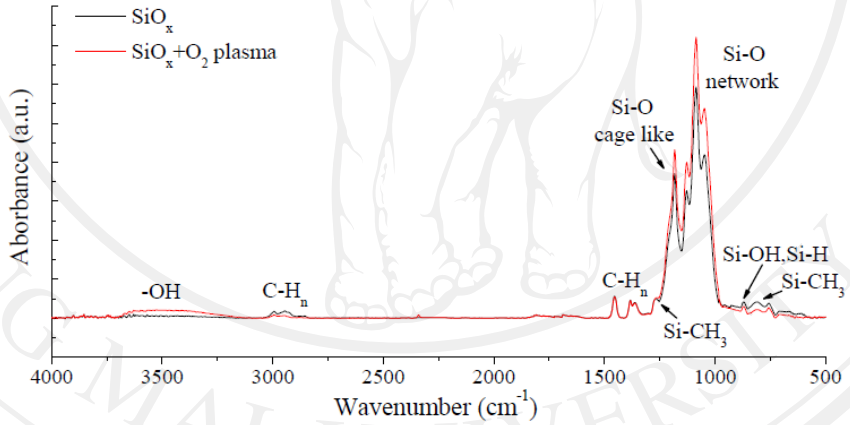

Figure 3. ATR- FTIR spectra of the as-deposited SiO_x and O_2-plasma treated SiO_x films.

The ATR-FTIR spectra of the as-deposited SiO_x film and O_2-plasma treated SiO_x film are show in Figure 3. The absorbance spectra of OMCTS were collected from 500-1350 cm^{-1} and compared with the spectral data of the known structures. In the PECVD of the films, a high ion current density enhanced the film density and hardness [10]. In this case, the Si-O network structure and Si-O cage-like structure showed very strong absorption bands in the range of 960-1250 cm^{-1}. The Si-O structure comprised Si-O-Si (1050 cm^{-1}), ring link Si-O-C (1085 cm^{-1}), open link Si-O-C (1128 cm^{-1}), and cage link Si-O-C (1180 cm^{-1}). The alkyl groups as $Si-CH_3$ and $-CH_n$ were found in the small region. The peaks at 754, 810, and 1268 cm^{-1} could be assigned to the Si-C stretching and the $-CH_3$ rocking modes as $Si-(CH_3)$ and $Si-(CH_3)_2$ [22]. The small peak at 874 cm^{-1} could be assigned to Si-OH and Si-H which indicated the incorporation of some moisture into the oxide films [23] which were related to the broad peak of -OH bond between 3150 and 3600 cm^{-1}. The peak between 2830 and 3025 cm^{-1} of the $-CH_n$ stretching bond consisted of $-CH_2$ and $-CH_3$. The $-CH_n$ peaks at 1360, 1379, and 1449 cm^{-1} could be assigned to $-CH_2$, $-CH_3$ and $-CH_4$, respectively [22]. It was found that after O_2-plasma treatment,

the -CH_n stretching bond and the Si-CH_3 bond decreased, whereas the -OH stretching bond increased. This implied that the O_2-plasma treatment reduced the carbon content of Si-O films, and hydrogen from moisture was incorporated into the oxide films and contributed to the polar surface to enhance the SiO_x wettability.

3.2. Cell culture

Cell attachment and proliferation of mouse fibroblast cells (L929) and mouse pre-osteoblast cells (MC3T3-E1) were observed in 1 day and 3-7 days, respectively, and the results are summarized in Figure 4. It showed both types of the cells attached on the as-deposited SiO_x films slightly more than on the O_2-plasma treated SiO_x films due to the lower BSA adsorption on the untreated films. The low BSA adsorptions resulted in the cell adhesion proteins more adsorbed on to the film surface, and thus the cells could have more attachment. But, both types of the cells proliferated on the O_2-plasma treated SiO_x films more than on the untreated as-deposited SiO_x films. Mouse pre-osteoblast cells proliferated slower than mouse fibroblast cells. The results indicated that the cell attachment depended on the protein adsorption on the surfaces, while the cell proliferation depended on the surface wettability.

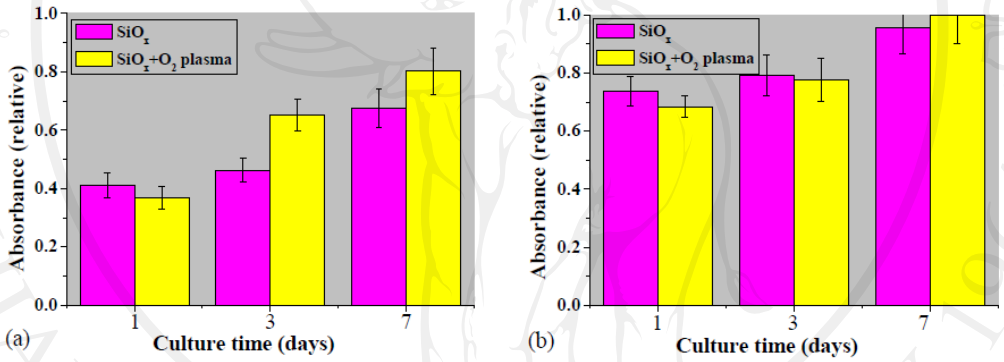

Figure 4. Relative absorbance of (a) L929 mouse fibroblast cells and (b) MC3T3-E1 mouse pre-osteoblat cells on the SiO_x and O_2-plasma treated SiO_x films measured by MTT assay after 1, 3, and 7 days, respectively.

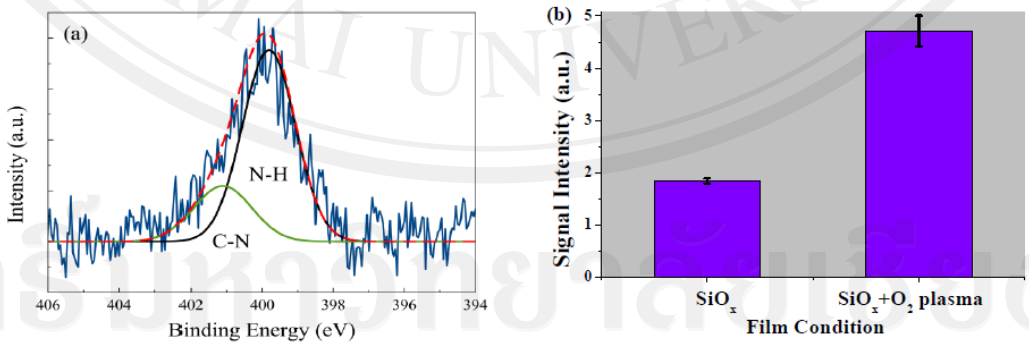

Figure 5. The concentration of the nitrogen bonds on BSA adsorbed on films SiO_x only and SiO_x treated with O_2-plasma measured by XPS. (a) An example of the original XPS spectrum with deconvoluted components. (b) The calculated N-signal intensity indicating the N concentration in the films.

3.3. Protein adsorption

Protein adsorption is a very complex process, depending on environment. There are three major factors: protein, surface and solution, and each factor depends on its properties. As several factors are present, it is quite difficult to focus on only a single factor. However, it may say correctly that the key factor of protein adsorption is the conformation change of proteins or peptides on substrate [24]. This is influenced by kinetic and thermodynamic considerations.

Applications of protein adsorption are almost related to blood plasma proteins. Alb is the most abundant protein in blood with a high concentration of 45 mg/ml, a molecular weight of 66 kDa, and an isoelectric point of 5.5 which has a negative charge in blood of pH 7.4. It is a globular protein in a soft protein type, which has a low internal stability in aqueous solution.

Generally, soft proteins adsorb on a hydrophobic surface rather than a hydrophilic surface, because the proteins tend to conserve their native structure on hydrophilic surface [25-28]. When biomaterials come into an aqueous solution, a water shell will form on the surface in a microsecond. Dehydration of the surface occurs in the next step, and the water structure forms hydrogen bonds with hydrophilic surface. On the hydrophilic surface, Alb will adsorb on the water layer with less tightly bond namely reversible bond. On the hydrophobic surface, water shell cannot form on the surface and Alb adsorbs on a water-free contact layer due to the hydrophobic effect with irreversible bond [29].

There have been many studies on controlling adsorption/desorption proteins to surface with the surface wettability. This study was focused on bovine serum albumin (BSA) adsorption onto SiO_x films with certain wettability. BSA was used to represent mammalian albumin. Some characteristics of BSA adsorption were investigated by XPS. Nitrogen peaks are caused by the presence of the amino acid sequence of BSA molecules. In the XPS spectrum the N1s peak was deconvoluted into two peaks, assigned to the N-H and C-N groups [30]. Figure 5 shows the concentration of the nitrogen bonds on BSA adsorbed on the SiO_x films and O-plasma treated SiO_x films measured by XPS. It is seen that the O-plasma-treated SiO_x films had more nitrogen than the untreated films, indicating the former absorbing more protein than the latter due to a lower energy band gap. The energy band gap has been rarely taken into account for a material surface factor of protein adsorption. Gandhiraman [31] studied the fibrinogen adsorption on $SiO_xC_yH_z$, TiOx and SiO-TiO films with the surface factors of wettability, roughness and energy band gap. They found that fibrinogen adsorption was the highest on the low energy band gap.

4. Conclusion

SiO_x films were deposited on PLA substrate using the PECVD technique and further treated with O_2-plasma to investigate the film surface wettability effect on the protein adsorption and cell attachment and proliferation. The O_2-plasma significantly enhanced the surface wettability of the SiO_x films without changing the thickness of the films but smoothing the surface morphology. Increase in the OH bond was responsible for the enhancement of the wettability due to hydrogen replacement and incorporation into the oxide films to contribute to the polar surface. BSA protein was more adsorbed on the hydrophilic SiO_x films treated by O_2-plasma with the low energy band gap, resulting in less cell attachment but cell-type-dependent cell proliferation, increased for the L929 mouse fibroblast cells but almost no changes for the MC3T3-E1 mouse pre-osteoblat cells. The results provide some hints for designing certain applications of SiO_x films on polymers in biomedicine.

Acknowledgements

This work was supported by the Institute for Plasma-Nano Materials, Center of Advanced Plasma Surface Technology, Sungkyunkwan University, Korea, the Department and Research Institute of Dental Biomaterials and Bioengineering, College of Dentistry, Yonsei University, Korea, the Thailand Center of Excellence in Physics, and the Graduate School of Chiang Mai University. We wish to thank Adcharaporn Boonma of the School of Mechanical Engineering, Institute of Engineering, Suranaree University of Technology for PLA films and Si-Eun Kim for assistance in cell culture.

References

[1] Chen H, Yuan L, Song W, Wu Z and Li D 2008 *Prog Polym Sci.* **33** 1059-87
[2] Goddard J M and Hotchkiss J H 2007 *Prog Polym Sci.* **32** 725
[3] Groth T and Altankov G 1996 *J Biomat Sci-Polym E.* **7** 305
[4] Yu Q, Zhang Y, Wang H, Brash J and Chen H 2011 *Acta Biomater.* **7** 1550-57
[5] Yang J, Bei J and Wang S 2002 *Biomaterials.* **23** 2607-14
[6] Jeyachandran Y L, Mielczarski J A, Mielczarski E and Rai B 2010 *J Colloid Interf Sci.* **341** 142
[7] Ryu G H, Yang W S, Roh H W, Lee I S, Kim J K, Lee G H, Lee D H, Park B J, Lee M S and Park J C 2005 *Surf Coat Tech.* **193** 64
[8] Huang C, Sun Y M, Tsai C Y, Wu S Y, Chang S C and Chang Y C 2012 *Surf Coat Tech.*
[9] Hayakawa T, Yoshinari M and Nemoto K 2004 *Biomaterials.* **25** 127
[10] Jin S B, Choi Y S, Kim Y J, Choi I S and Han J G 2010 *Surf Coat Tech.* **205** S139-43
[11] Chaiwong C, Rachtanapun P, Sarapirom S and Boonyawan D 2012 *Surf Coat Tech.*
[12] Jin S B, Choi Y S, Choi I S and Han J G 2011 *Thin Solid Films.* **519** 6763-68
[13] Satriano C, Marletta G and Kasemo B 2008 *Surf Interface Anal.* **40** 656
[14] Mangindaan D, Yared I, Kurniawan H, Sheu J R and Wang M J 2012 *J Biomed Mater Res A.* **100A** 3177-88
[15] Noh H and Vogler E A 2007 *Biomaterials.* **28** 422
[16] Rudawska A and Jacniacka E 2009 *Int J Adhes Adhes.* **29** 457
[17] Żenkiewicz M 2007 *JAMME.* **24** 145
[18] Jian Yang J B, Shenguo Wang 2002 *Biomaterials.* **23** 2607-14
[19] Vanea E and Simon V 2011 *Applied Surface Science.* **257** 2346-52
[20] Gruian C, Vanea E, Simon S and Simon V 2012 *BBA-Protein Proteomic.* **1824** 881
[21] Bacakova L, Filova E, Parizek M, Ruml T and Svorcik V 2011 *Biotechno Adv.* **29** 767
[22] Kim C Y, Navamathavan R, Lee H J and Choi C K 2008 *Surf Coat Tech.* **202** 5688-92
[23] Matilainen A, Britun N, Jin S B and Han J G 2010 *Surf Coat Tech.* **205** S300-04
[24] Mu Y 2011 *Phys Rev E.* **84** 031906
[25] D'Sa R A, Burke G A and Meenan B J 2010 *Acta Biomater.* **6** 2609-20
[26] Cole M A, Voelcker N H, Thissen H and Griesser H J 2009 *Biomaterials.* **30** 1827-50
[27] Vogler E A 2012 *Biomaterials.* **33** 1201-37
[28] Azioune A, Siroti F, Tanguy J, Jouini M, Chehimi M M, Miksa B and Slomkowski S 2005 *Electrochim Acta.* **50** 1661-67
[29] Werner C, Eichhorn K J, Grundke K, Simon F, Grählert W and Jacobasch H J 1999 *Colloid Surface A.* **156** 17
[30] Indest T, Laine J, Kleinschek K S and Zemljič L F 2010 *Colloid Surface A.* **360** 219
[31] Gandhiraman R P 2007 *PECVD silicon and titanium based coatings to enhance the biocompatibility of blood contacting biomedical devices* Dublin City University (Dublin City) 110

Applied Surface Science 310 (2014) 42–50

Contents lists available at ScienceDirect

Applied Surface Science

journal homepage: www.elsevier.com/locate/apsusc

Effect of surface modification of poly(lactic acid) by low-pressure ammonia plasma on adsorption of human serum albumin

S. Sarapirom[a], L.D. Yu[a,b,*], D. Boonyawan[a,b], C. Chaiwong[a,b,*]

[a] Plasma and Beam Physics Research Facility, Department of Physics and Materials Science, Faculty of Science, Chiang Mai University, Chiang Mai 50200, Thailand

[b] Thailand Center of Excellence in Physics, Commission on Higher Education, 328 Si Ayuthaya Road, Bangkok 10400, Thailand

ARTICLE INFO

Article history:
Received 21 November 2013
Received in revised form 20 March 2014
Accepted 20 March 2014
Available online 30 March 2014

Keywords:
Poly(lactic acid) (PLA)
Ammonia (NH_3) plasma
Human serum albumin (HSA)
Adsorption
Polar group

ABSTRACT

The final goal of the study was to promote understanding of mechanisms involved in cell attachment on biomedical polymer poly(lactic acid) (PLA). As the cell attachment on the material surface was preceded by blood protein adsorption which would critically affect subsequent cell adhesion, for the clinic application purpose, human serum albumin (HSA) was used in the investigation on its adsorption on PLA, which was however treated by low-pressure ammonia (NH_3) plasma. The NH_3-plasma-treated PLA was found to adsorb less HSA than the untreated PLA. The PLA was characterized using various techniques such as atomic force microscopy, contact angle and surface energy analysis and x-ray photoelectron spectroscopy. All of the characterization results indicated that due to NH_3-plasma-induced polar groups the PLA enhanced its hydrophilicity which in turn inhibited the HSA adsorption. The decreased HSA adsorption would consequently increase the cell attachment because of the cell adhesion barrier reduced.

Introduction

Poly(lactic acid) (PLA) is one of biodegradable polymers that has been increasingly important in biomedical applications, such as drug delivery, artificial tissues, implant organs, and tissue engineering [1–4]. However, its applications in artificial tissues and organs are limited due to poor cell attachment to the surface attributed to its hydrophobicity and lack of reactive side chain groups, but mechanisms in deeper levels have been yet unclear. In the case of human cell attachment on the artificial materials cell adhesion was preceded by adsorption of cell adhesion proteins to the material surface. The adsorbed protein on the surface would form a barrier layer to subsequent cell attachment, that is, the more blood protein adsorbed, the less cells attached. The mechanisms of protein attachment on the material surfaces actually depend on the surface, protein and environment such as diffusion coefficient, molecular mass, electrical charge, polarity and pH [5–7]. Several methods have been developed to modify the surface of PLA [6,8,9]. Among them, plasma treatment is an effectivemethod to incorporate the desired groups or chains onto the surface of PLA. Gas plasmas such as CO_2, O_2, N_2, H_2 and NH_3 can create reactive sites such as hydroxyl (–OH), carboxyl (–COOH) or amino groups ($–NH_2$) on the polymer surface [10–14]. Ammonia (NH_3) plasma was demonstrated to be able to improve the hydrophilicity and biocompatibility of PLA more effectively than other gas plasmas [12] with modifying the surface morphology and increasing amino groups while decreasing the contact angle [15]. Mechanisms involved in the promotion of cell adhesion and proliferation by ammonia plasma were also studied and confirmed that wettability, chemical composition, morphology and charge of PLA were important parameters that controlled protein adsorption, cell interaction, and biocompatibility [10,14,16]. Recently, a number of researchers have explored surfaces that enhance specific protein adsorption or cell affinity. For example, Kunzler et al. [17] found that osteoblasts preferred rougher surfaces whereas fibroblasts favoured smoother surfaces. Ying et al. [18] showed that bovine serum albumin (BSA) was preferentially adsorbed onto a hydrophobic surface. They also investigated the competitive adsorption of albumin against collagen and found that albumin was adsorbed onto the hydrophobic surface better than collagen. Although there have been many studies of protein adsorption onto surface of polymeric materials, a complete picture of the mechanisms has not yet been provided.

When a material is inserted into a human body, protein adsorption is the first step to take place. Albumin, the most abundant

* Corresponding authors at: Tel.: +66 53 942464; fax: +66 53 222776.
E-mail addresses: yuld@thep-center.org (L.D. Yu), cchwng@gmail.com (C. Chaiwong).

http://dx.doi.org/10.1016/j.apsusc.2014.03.141
0169-4332/

plasma protein, is the first protein to adsorb on the implant surface and then it can be replaced by immunoglobulin-G (IgG), which in turn is displaced by fibrinogen (Fb) and higher molecular weight proteins [19]. Therefore, the adsorption of cell attachment proteins and the subsequent attachment of cells are controlled by the affinity of albumin. In this work we studied the adsorption of human serum albumin (HSA) on PLA surface, aiming at finding out relationships between the PLA surface properties which were altered by ammonia plasma treatment and adsorption of HSA for revealing relevant mechanisms in cell attachment.

Experimental

Materials

PLA films of the thickness 50 μm (NatureWork® with L/D ratios from 24:1 to 30:1) were made in the standard calendering process by the School of Mechanical Engineering, Institute of Engineering, Suranaree University of Technology, Thailand. Samples of the PLA films were prepared in 3 cm × 12 cm strips, wiped with 95% ethanol and stored in a desiccator at 25 ± 2 °C for 24 h prior to the plasma treatment.

Plasma treatment

NH_3-plasma treatments were carried out using a home-made 13.56-MHz inductively coupled plasma reactor [20]. Film samples were put into the quartz cylinder of the plasma reactor and then the cylinder was evacuated to a base pressure of 0.01 Pa. To remove residues, the film samples were first sputtered by Ar plasma at 3.3 Pa and a radiofrequency (RF) power of 50 W for 1 min. After that, the films were treated with NH_3 plasma discharged at RF powers of 50 W, 75 W, and 100 W, respectively. The NH_3 gas pressure was controlled at 1.65 Pa and the treatment time was fixed for 10 min. Optical emission spectroscopy (OES) was used to observe the active plasma species.

Protein adsorption

The HSA (lyophilized powder, A1653) and 0.01-M phosphate buffered saline (PBS) (NaCl –0.138 M, KCl – 0.0027 M) in pH 7.4 at 25 °C were purchased from the Sigma–Aldrich Corporation, Germany. The HSA solution (0.5% W/V in water) was drop on the 1 cm × 1 cm Si wafer and left at room temperature for 12 h before x-ray photoelectron spectroscopy (XPS) analysis of the pure HSA. Strips of untreated, Ar-pre-treated and NH_3-plasma-treated PLA films were cut into 1 cm × 1 cm. Three replications of each condition were placed into wells of a 4-well plate. The protein was immobilized onto the films by adding 1 ml of HSA solution (0.5% W/V in PBS) into each well and then the films were incubated for 20 min on a rocking shaker at room temperature. After incubation, the films were washed in distilled water for 20 min, first soaking and then rinsing 3 times. For observation and analysis of the protein adsorbed films, the films were dried in a new plate and left at room temperature for 12 h before the atomic force microscopy (AFM) observation and XPS analysis.

Film characterizations

Atomic force microscopy (AFM)

The surface morphology of the untreated (control), Ar-pre-treated, NH_3-plasma treated and protein adsorbed PLA films in a size of 1 cm × 1 cm was observed using an atomic force microscope (AFM) (SHIMADZU SPM-9500 J2, Japan). Three replicates of each condition were adopted. Images were acquired in the tapping mode and using silicon tips with a scan rate of 2 Hz in air and a scan size of 1 μm × 1 μm. Three different regions were scanned on each sample. The image analysis was carried out using a Di Nanoscope III version 5.12r3 software.

Contact angle and surface energy

Static contact angles were measured using 2-μl droplets of deionised water and diiodomethane (CH_2I_2), respectively, at room temperature. Three replicates of the untreated (control), Ar-pre treated and NH_3-plasma treated PLA were cut into 2 cm × 4 cm. The measurement was operated at 5 different regions on each sample. Images of the fluid drops were captured and analyzed by using an image analysis software. The surface energy was calculated using the Owens–Wendt equations [21,22]:

$$\gamma_W\left(1+COS\theta_W\right)=2\sqrt{\gamma_S^d\gamma_W^d}+2\sqrt{\gamma_S^p\gamma_W^p} \quad (1)$$

$$\gamma_D\left(1+COS\theta_D\right)=2\sqrt{\gamma_S^d\gamma_D^d}+2\sqrt{\gamma_S^p\gamma_D^p} \quad (2)$$

where γ is the surface energy, the superscripts d and p represent the dispersive component and the polar component of the surface energy, respectively, the subscripts W, D and S are the water, diiodomethane and solid components, respectively, θ is the contact angle of the surface energy, θ_W is the contact angle of water, and θ_D is the contact angle of diiodomethane. For water, γ_W = 72.8 mJ/m^2, γ_W^d = 22.1 mJ/m^2, and γ_W^p = 50.7 mJ/m^2. For diiodomethane, γ_D = 50.8 mJ/m^2, γ_D^p = 44.1 mJ/m^2, and γ_D^d = 6.7 mJ/m^2 [10].

X-ray photoelectron spectroscopy (XPS)

X-ray photoelectron spectra of untreated, NH_3-plasma treated and HSA protein adsorbed PLA films as well as pure HSA (on Si substrate) were obtained using an AXIS ULTRA XPS spectrometer (KRATOS analytical, UK). The samples for XPS analysis were prepared in the same size of the substrates (1 × 1 cm^2) and the same volume of HSA. The monochromatic Al Kα x-ray source was operated at an anode power 150 W. Survey spectra were acquired from 0–1200 eV with pass energy of 80 eV and a step size of 1 eV. The core-level spectra (high-resolution spectra) were obtained with pass energy of 20 eV and a step size of 0.1 eV. Elemental compositions were calculated from peak areas obtained from the survey spectra. Three replicates of each condition were analyzed. A low-energy electron flood gun was used to compensate for surface charging on the insulating films. All XPS peaks were referenced to a C_{1S} signal at a binding energy of 284.6 eV, corresponding to the C–C and C–H bonds in hydrocarbons. The peaks were deconvoluted into Gaussian components with the same full width at haft maximum (FWHM) to gain the insight into the bonding.

Results and discussion

Plasma diagnostics

The spectrum of NH_3 plasma was observed by OES in a range of 200–800 nm. The prominent lines observed were the NH line at 336.7 nm, the N line at 315.9 nm, the N_2 line at 357.7 nm, the N_2^+ line at 391.4 nm, the CN line at 388.9 nm, the H_β line at 486.2 nm, the H_2 band at 546.0 nm and the H_α line at 655.7 nm [23–25]. The NH, N_2, and CN species increased with increasing of the RF power.

Protein adsorption

HSA is a heart-shaped protein with a molecular weight of 66 kDa and has a negative charge in pH 7.4 of blood [26]. AFM was used to observe the adsorption of HSA onto the surfaces of the untreated and NH_3-treated samples, as shown in Fig. 1. There was no globular structure detected by the AFM, indicating that HSA

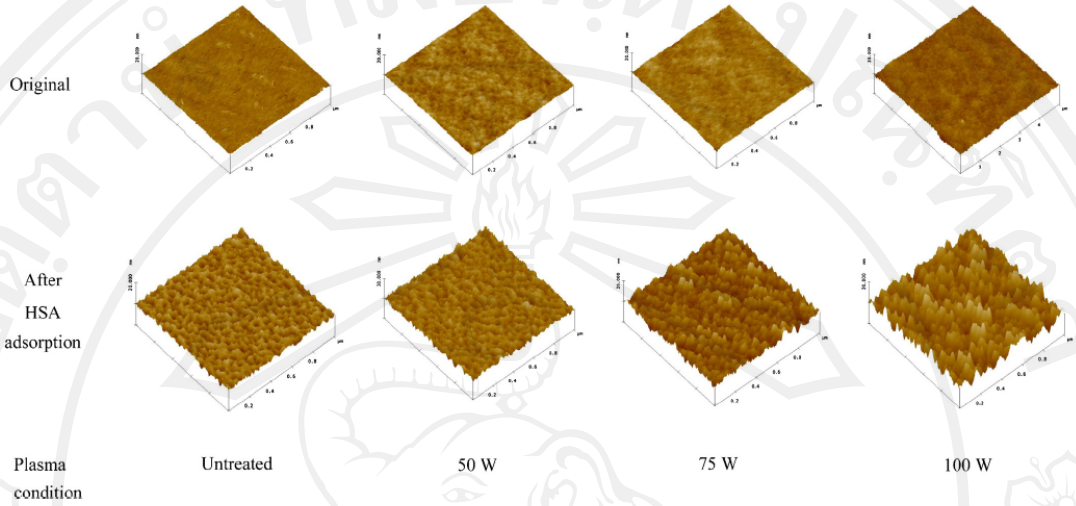

Fig. 1. AFM images of untreated PLA and NH_3-plasma treated PLA with various RF powers before and after protein adsorption.

Table 1
The roughness of untreated PLA and NH_3-plasma treated PLA with RF powers of 50 W, 75 W, and 100 W before and after HSA adsorption, measured by AFM. The "change" refers to a difference in roughness between the treated and untreated surfaces.

RF Power (W)	RMS Roughness (nm)/change			
	Before HSA adsorption	±S.D.	After HSA adsorption	±S.D.
0 (Untreated)	0.12/0	0.01	1.27/0	±0.07
Ar-pre treated	0.15/+0.03	±0.03	1.30/+0.03	±0.03
50 W	0.25/+0.13	±0.01	1.34/+0.07	±0.04
75 W	0.26/+0.14	±0.02	2.26/+0.99	±0.10
100 W	0.32/+0.20	±0.03	3.10/+1.83	±0.08

were uniformly distributed over the surface of the samples without aggregation. The root-mean-square (rms) roughness (Table 1) of the HSA-covered plasma-treated samples was higher than that of the HSA-covered untreated samples and the roughness clearly increased as increasing of the RF power of the plasma generation. The smoother morphology of the HSA-covered untreated sample surface was due to a higher or even full coverage of HSA, whereas the coarser morphology was caused by a lower HSA coverage which led to some material surface areas uncovered, resulting from protein aggregation into islands [27]. The increased surface roughness also indicated changes in the HSA conformation and hence biological activity [28]. The surface roughness change qualitatively indicated that HSA adsorption was reduced on the NH_3-plasma treated PLA surface compared with that on the untreated PLA surface. XPS analysis as described later provided a semi-quantitative evaluation on the HSA adsorption reduction.

Film characterizations

Surface morphology

Surface morphology of the films was observed by AFM and roughness data were obtained from different regions on each sample. Fig. 1 shows the AFM images of untreated and NH_3-plasma treated PLA surfaces and the AFM-measured rms roughness of the samples was in the range of 0.1–0.3 nm, as shown in Table 1. It is seen that the plasma treatment caused the surface roughness to increase doubly and the roughness increase was little dependent on the plasma generation power. There were some small changes in the magnitude of the grain structure. Fine grain structures of the surfaces were observed after the NH_3-plasma treatment. The result on the roughness increase is in agreement with a previous reported one which showed the surface of poly(L-lactic acid) (PLLA) became rougher form 22.32 nm to 37.50 nm (nearly double) after NH_3 plasma treatment with an RF power of 100 W for 2 min [15].

Contact angle and surface energy

Table 2 shows the results of the contact angle measurements. The water contact angle of the untreated sample was 69.0°. After the NH_3-plasma treatment, the water contact angles decreased, with increasing RF powers, to the lowest water contact angle about 15°. The contact angles of CH_2I_2 were also decreased after the plasma treatment. Table 2 also shows the components of surface energy of the samples calculated using the Owens–Wendt equations (Eqs. (1) and (2)). The polar component of surface energy comprises all other interactions due to non-London forces. Polar molecules interact with dipole forces and hydrogen bonds. The dispersive

Table 2
The contact angle and surface energy of untreated, Ar pre-treated and NH_3 plasma treated PLA with RF powers of 50 W, 75 W, and 100 W. Treatment time was 10 min.

RF Power (W)	Contact angle (degree) ±S.D.		Surface energy (mJ/m²)		
	θ H_2O	θ CH_2I_2	γ_s^p	γ_s^d	γ_s
0 (Untreated)	69.0 ± 1.9	39.1 ± 2.0	11.0	30.3	41.3
Ar-pre treated	52.2 ± 1.7	31.7 ± 1.1	23.1	27.1	50.2
50 W	20.0 ± 1.0	32.9 ± 1.9	50.4	18.2	68.6
75 W	15.0 ± 1.0	30.3 ± 2.2	51.7	18.7	70.5
100 W	15.5 ± 0.7	32.1 ± 1.3	52.4	18.0	70.4

or non-polar components of surface energy result from molecular interactions due to London forces [25]. The polar components of surface energy are seen significantly increased after the plasma treatments. Although the Ar pre-treatment contributed some, it was not as much as the NH_3-plasma treatment did. On the contrary, the dispersive component decreased. The total surface energy was obviously higher after the plasma treatments, indicating that the surface of PLA became more hydrophilic. A decrease in the contact angle and an increase in the surface energy of PLA with the contribution of the polar component due to NH_3 plasma treatment were previously reported [12]. The hydrophilicity of the PLA films was improved by the NH_3-plasma treatment due to increased polarity, as demonstrated by greater polar components present in the total surface energy. This could result from the incorporation of polar groups such as amine or amide group on the surface.

XPS

The chemical compositions of the untreated PLA and the NH_3-treated PLA were analyzed and obtained from XPS. Fig. 2 shows survey scans of the PLA samples. The spectrum of the untreated PLA shows only C_{1s} and O_{1s} peaks (Fig. 2a), whereas N_{1s} peaks (400 eV) appeared in the spectra of all the NH_3-plasma treated samples (Fig. 2c–e) but not in that of the untreated sample (Fig. 2a). To study the incorporation of N into PLA, the N_{1s} peaks of the samples were deconvoluted as shown in Fig. 3. After fitting of the N_{1s} peak with the same FWHM four components corresponding to nitrogen were found. The peaks appearing at 398.8 eV, 399.8 eV, 401.2 eV and 402.8 eV were assigned to the imine group (C=N), amine group (C–NH), amide group (C=O–NH) and ammonium species (NH_3^+) [28–30], respectively. The main component was amine group and the ammonium species was found after NH_3-plasma treatment with an RF power of 75 W and 100 W. The C_{1s} peak from the untreated PLA was deconvoluted into four peaks at 284.6 eV (C–H/C–C), 286.6 eV (C–OH/C–O–C), 288.9 eV (C=O/O–C=O) and 289.7 eV (COO), as shown in Fig. 4a. The deconvoluted C_{1s} peak

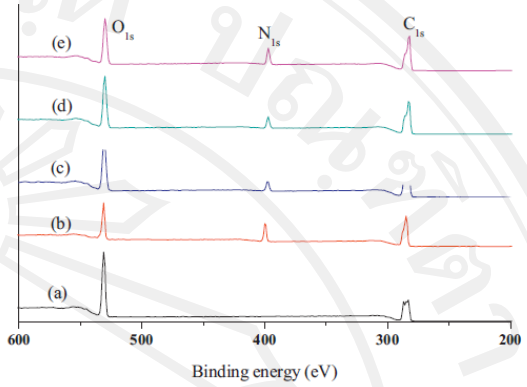

Fig. 2. XPS survey spectra of (a) untreated PLA, (b) pure HSA, and NH_3-plasma treated PLA with RF powers of (c) 50 W, (d) 75 W and (e) 100 W.

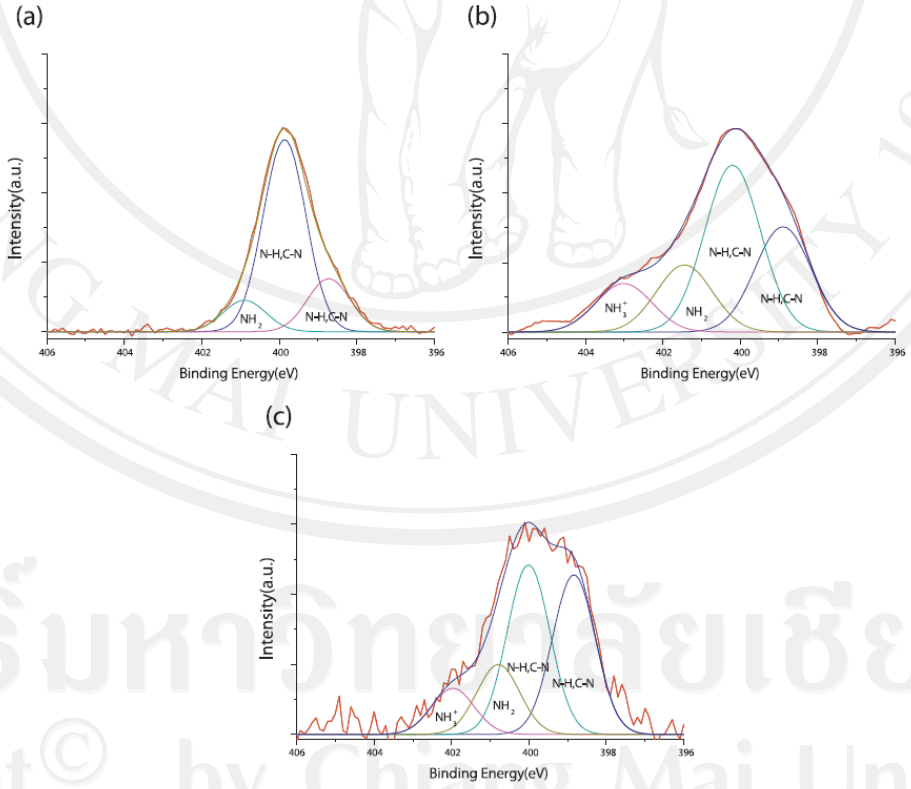

Fig. 3. Deconvoluted N_{1s} peaks of XPS spectra from NH_3-plasma treated PLA with RF powers of (a) 50 W, (b) 75 W, and (c) 100 W.

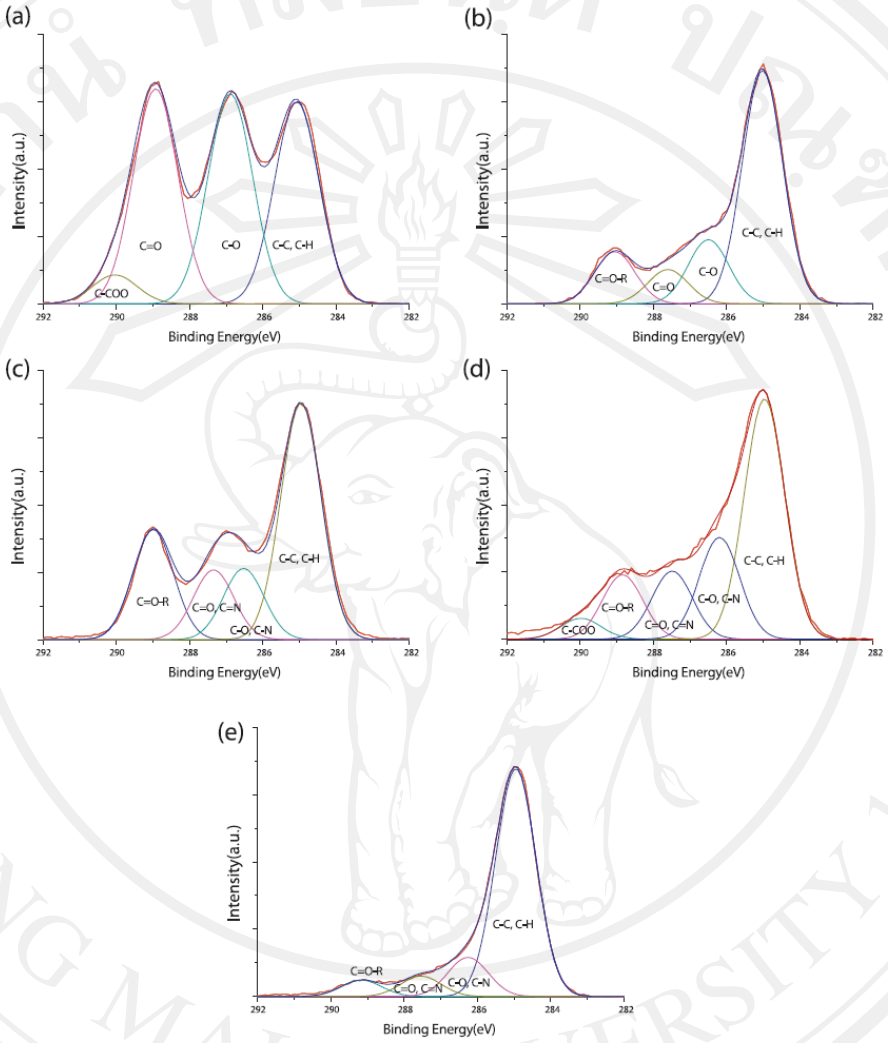

Fig. 4. Deconvoluted C_{1s} peaks of XPS spectra of (a) untreated PLA, (b) Ar-pre-treated, and NH_3-plasma treated PLA with RF powers (c) 50 W, (d) 75 W, and (e) 100 W.

from the NH_3 treated samples, as shown in Fig. 4b–e, involves a peak at 284.6 eV associated to C–H/C–C bonds, a peak at 286.6 eV due to C–NH and C–O bonds, a peak at 287.5 eV due to C=O and C=N bonds, a peak at 288.2 eV attributed to C=O, HN–C=O, N–C=N bonds, and a peak at 289.7 eV owing to O=C–O(H,R) bond [28–32]. The atomic compositions of C, O, and N are shown in Table 3. While the C concentrations of the plasma-treated samples remained similar to that of the untreated sample, the O concentrations of the treated samples decreased compared with that of the untreated sample. This could be owing to the fact that grafted N-containing groups substituted oxygen containing functional groups. Finally, the O/C ratio decreased from about 0.60 to 0.37 and the N/C ratio

Table 3
Atomic concentrations of chemical components of untreated, Ar pre-treated and NH_3-plasma treated PLA with RF powers of 50 W, 75 W, and 100 W. Treatment time was 10 min.

RF Power (W)	%C ±S.D.	%O ±S.D.	%N ±S.D.	O/C	N/C
0 (Untreated)	62.39 ± 0.26	37.61 ± 0.41	0.00 ± 0.00	0.603	0.000
Ar pre-treated	63.20 ± 0.38	36.80 ± 0.73	0.00 ± 0.00	0.580	0.000
50 W	65.41 ± 0.66	27.43 ± 0.96	7.15 ± 0.22	0.419	0.109
75 W	65.64 ± 0.52	26.54 ± 0.63	7.82 ± 0.46	0.404	0.119
100 W	65.22 ± 0.31	23.98 ± 0.34	10.80 ± 0.52	0.368	0.166

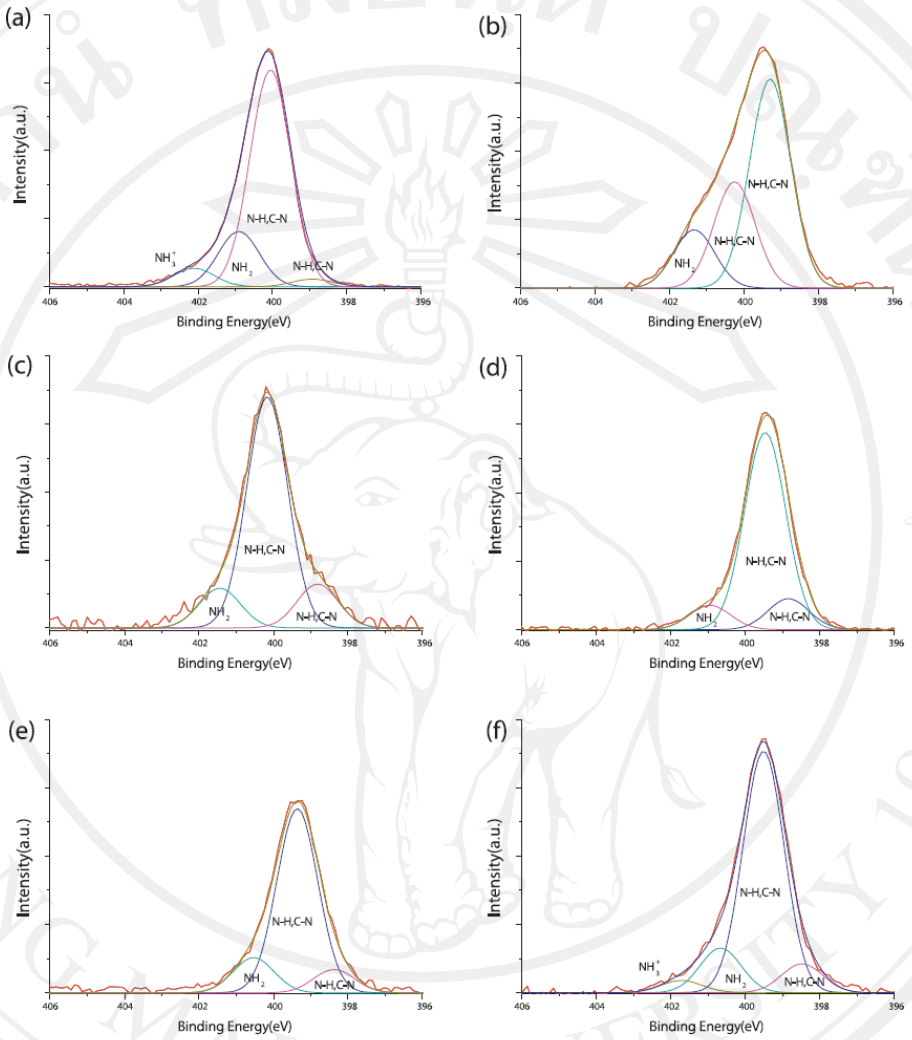

Fig. 5. Deconvoluted N_{1s} peaks of XPS spectra from (a) pure HSA, and HSA-adsorbed (b) untreated PLA, (c) Ar-pre-treated and NH_3-plasma treated PLA with RF powers of (d) 50 W, (e) 75 W, and (f) 100 W.

increased from 0 to 0.17 when the RF power was increased from 0 to 100 W. These results are similar to previously reported O/C ratio decrease from 0.46 to 0.34 and N/C ratio increase from 0 to 0.10 obtained also from XPS analysis [12,28]. Decreases in O/C ratio and increases in N/C ratio could contribute to the reduction of water contact angles. N-containing groups such as the amine group were incorporated into PLA and thus contributed to the polar surface to improve the PLA wettability.

XPS was also used to investigate the HSA attachment characteristics on the samples. In this case, the nitrogen peak appearing in the spectrum was not only caused by the NH_3-plasma treatment introduced nitrogen but also by the presence of the amino acid sequence of the HSA molecules. As shown in Fig. 5, the N_{1s} peak was deconvoluted into four peaks, assigned to imine, amine, amide and amino groups (NH_3^+), respectively. In pure HSA, amine group was the main structure, the same as in the plasma-treated PLA films, but in the untreated PLA films the main structure was imine group. A high resolution analysis of the C_{1s} peak from pure HSA (Fig. 6a) showed strong peaks of amino (C–NH) and peptide bound (C═O–NH). After HSA adsorption the PLA film had more amide bond, similar to the Ar-pre-treated and NH_3-plasma treated PLA with 50-W RF power. For NH_3-plasma treated PLA with RF power 75 W and 100 W amide bonding and amine bonding were found decreasing. This indicated that HSA bounded on the surface with the carboxyl and amino groups did not interact strongly with the surface [29]. Table 4 shows the XPS-analyzed atomic concentrations of C, O and N in the untreated and the NH_3-treated samples after the protein adsorption. It is seen that after HSA adsorption the N concentration decreased whereas the others remained similar. Compared with the N data in Table 3, where the N concentration increased due to N from ammonia incorporated into PLA, the opposite trend of the N concentration change could only indicate

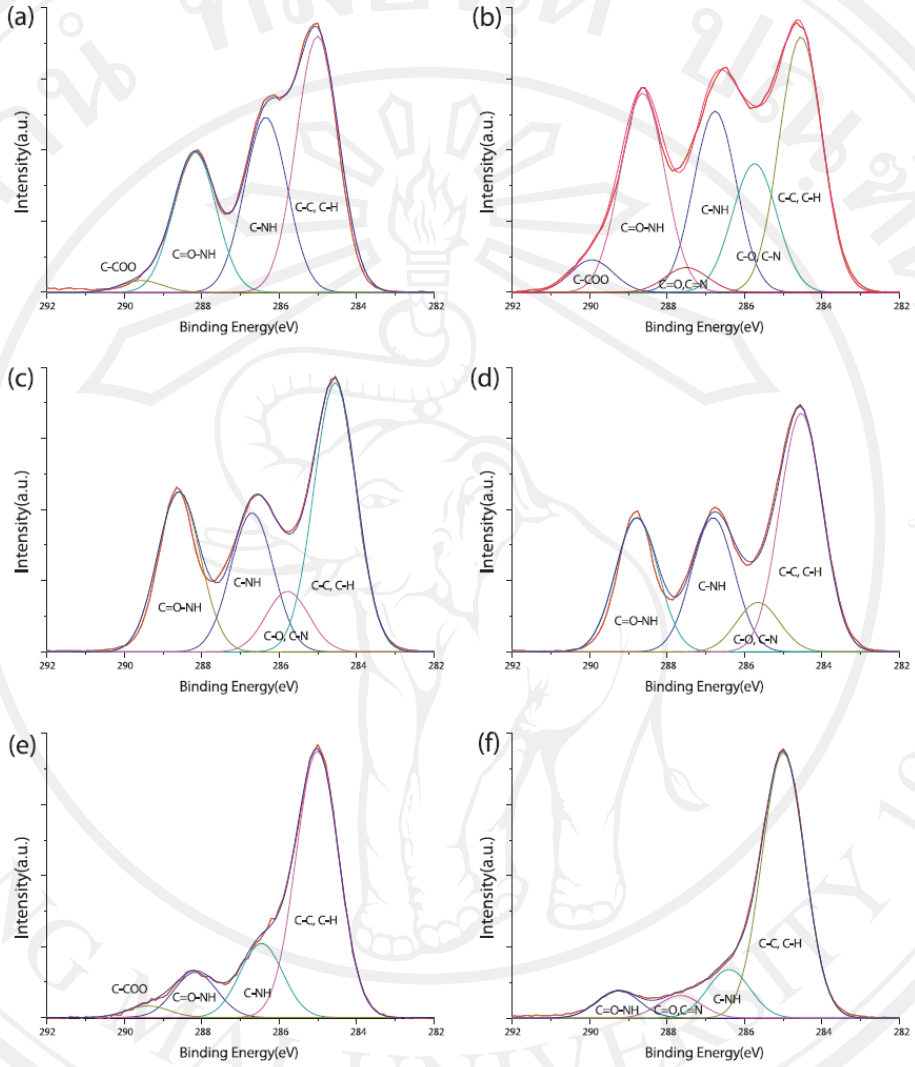

Fig. 6. Deconvoluted C_{1s} peaks of XPS spectra of the (a) pure HSA and HSA-adsorbed on (b) untreated PLA, (c) Ar-pre-treated and NH_3-plasma treated PLA with RF powers of (d) 50 W, (e) 75 W, and (f) 100 W.

the plasma-treated PLA adsorbed less HSA which contained nitrogen. We then tried to quantify the above qualitative observation with respect to the relative content of N of HSA, which represented relative quantity of HSA adsorbed on PLA, as described below.

From XPS measurement, it is known from Tables 3 and 4 that C%, O% and N% in pure PLA and pure HSA are 62.39 and 66.62, 37.61 and 17.77, and 0 and 15.60, respectively. Assuming that the two materials are homogeneously mixed together, the averages of the three components should be 64.51, 27.7 and 7.8, respectively. But, the actually measured data shown in Table 4 from the real HSA-on-PLA sample are 64.84, 30.12 and 5.03, respectively. For the real sample, the measured C is almost the same that previously assumed, whereas the measured O is more and so the measured N is less than assumed. In the real XPS measurement, HSA is on the top of PLA, and so the XPS signal from PLA might be blocked by HSA in certain degrees. The energy of 1s electron of C is the lowest, about 270 eV, while that of O is the highest, about 530 eV. So, the C XPS signal from PLA does not readily pass through the HSA top layer to be detected, whereas that of O does. This is why the measured O is higher but the measured C is not much different from that the assumed. Because of the higher O percentage, the measured N concentration becomes lower. From this observation, the data in Table 4 should be reasonable. Therefore, the data in Table 4 were used to estimate the amount of N and thus the amount of HSA under various conditions. As the measured N concentration in the case of NH_3-plasma treated samples contained N from plasma-treated PLA as shown in Table 3, the amount of N from plasma-treated PLA should be subtracted. But, how much N from the plasma-treated PLA involved in the measured N concentration from HSA-on-PLA is unknown due to the fact that how much

Table 4
Atomic concentrations of chemical components of pure HSA, HSA-adsorbed untreated, Ar pre-treated and NH_3-plasma treated PLA with RF powers of 50 W, 75 W, and 100 W, respectively, analyzed by XPS. Treatment time was 10 min.

RF Power (W)	%C ±S.D.	%O ±S.D.	%N ±S.D.	O/C	N/C
Pure HSA	66.62 ± 0.45	17.77 ± 0.40	15.60 ± 0.27	0.267	0.234
0 (Untreated)	64.84 ± 0.67	30.12 ± 0.87	5.03 ± 0.69	0.465	0.078
Ar pre-treated	64.86 ± 0.26	30.13 ± 0.41	5.01 ± 0.46	0.465	0.077
50 W	65.64 ± 0.66	30.30 ± 0.73	4.27 ± 0.52	0.462	0.065
75 W	65.98 ± 0.52	30.17 ± 0.63	3.85 ± 0.34	0.457	0.058
100 W	65.89 ± 0.31	29.84 ± 0.34	4.27 ± 0.25	0.453	0.065

N signal from PLA able to pass through the HSA layer to be detected is unknown. Therefore, in order to estimate semi-quantitatively relative result, it is provided that the measured N concentration in the plasma-treated PLA as shown in Table 3 is totally involved in the measured N concentration from HSA-on-PLA. So, the calculation is then (%N in Table 4)[1–(%N in Table 3)] followed by normalization using the %N of the control (HSA-on-untreated PLA) as 100%. The result is shown in Fig. 7. Although the result is not absolute, it relatively shows a trend of the change in the N content with the sample treatment condition in a semi-quantitative manner. It is seen from the result that the nitrogen and thus also the adsorbed HSA decreases after NH_3 plasma treatment of the PLA substrate and roughly it decreases as increasing of the plasma power.

Discussion

All of the characterization data demonstrated that the NH_3 plasma treatment of the PLA surface resulted in an enhancement of hydrophilicity of the polymer surface from an originally more hydrophobic surface. The NH_3-plasma treatment enhances the surface energy and hydrophilicity by introducing nitrogen and oxygen functional groups onto the surface [12,15,28]. The protein attachment results meant that HSA was more strongly bound to the hydrophobic surface of the untreated PLA samples than to the hydrophilic PLA surface due to NH_3-plasma treatment. Normally, hydrophobic interactions are strong and thus responsible for protein attachment, whereas hydrophilic interactions with water molecules are much stronger than with proteins and hence a hydrophilic surface can hardly hold the protein [25]. In an aqueous environment, proteins tend to adopt either a hydrophobic surface or a hydrophilic surface but in different manners. Proteins can be irreversibly bound to a hydrophobic surface through the dehydration of the interface and undergoing conformation changes on hydrophobic part at the substrate surface [33]. In our case, HSA was more strongly bound to the hydrophobic surface of the untreated PLA because of dehydration during the interaction between the hydrophobic surface and HSA [34]. Thus, the HSA bound on the untreated more hydrophobic surface of PLA could not be removed by the rinsing procedure. On the other hand, HSA could be associated with the hydrophilic surface of the NH_3-treated PLA through the hydration layer and retained its original conformation. Hence, it was reversibly bound and could be washed off. As the surface had been washed with distilled water prior to XPS analysis, the protein left on the surface was considered to be irreversibly bound. The XPS analysis revealed that the polar groups containing nitrogen and oxygen were incorporated into the PLA surface to increase the surface energy of the PLA. The difference in adsorption of the HSA on hydrophobic and hydrophilic surfaces finally affects the cell attachment. HSA prefers binding to less oxygenated and more hydrophobic surfaces to form a barrier layer which thus makes subsequent cell attachment difficult. To improve cell attachment on the biomedically applied PLA, ammonia plasma treatment is then an effective choice in increasing the material surface hydrophilicity to reduce the HSA adsorption.

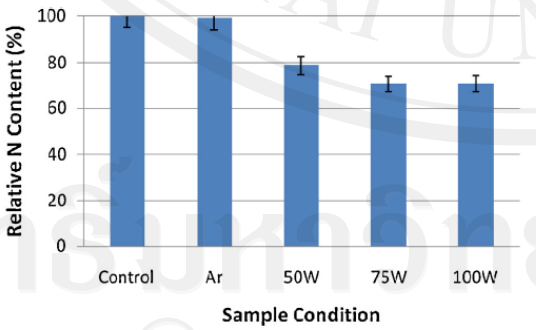

Fig. 7. Relative content of N in HSA-adsorbed untreated PLA (marked as Control), Ar-pre-treated PLA (marked as Ar), and NH_3-plasma treated PLA with power of 50 W (marked as 50 W), 75 W (marked as 75 W), and 100 W (marked as 100 W), respectively.

Conclusion

HSA adsorption on the surface of PLA was investigated for understanding mechanisms involved in cell attachment on the polymer and eventually looking for a solution to limited cell attachment on the polymer. Two types of PLA surfaces were tested, i.e. untreated PLA and NH_3-plasma treated PLA. HSA was adsorbed less on the plasma-treated PLA than on the untreated PLA. The material characterizations demonstrated that NH_3-plasma treatment raised the surface hydrophilicity of the PLA films due to the polar groups such as amines or amides. The HSA had a higher adsorption preference to non-polar surfaces than polar surfaces. The hydrophilic surface of PLA induced by NH_3 plasma would benefit to cell adhesion and enhance cell attachment since albumin was loosely bound on the surface and could thus be replaced by larger cell attachment proteins such as fibronectin, vitronectin and collagen which are the components of the extracellular matrix.

Acknowledgements

The work was supported by the Thailand Center of Excellence in Physics and Chiang Mai University. We wish to thank A. Boonma for PLA films, and C. Sriprom and K. Prakrajang for XPS analysis.

References

[1] M. Sokolsky-Papkov, K. Agashi, A. Olaye, K. Shakesheff, A.J. Domb, Polymer carriers for drug delivery in tissue engineering, Adv. Drug Deliver. Rev. 59 (2007) 187–206.
[2] M. Sabir, X. Xu, L. Li, A review on biodegradable polymeric materials for bone tissue engineering applications, J. Mater. Sci. 44 (2009) 5713–5724.
[3] M.P. Prabhakaran, J.R. Venugopal, S. Ramakrishna, Mesenchymal stem cell differentiation to neuronal cells on electrospun nanofibrous substrates for nerve tissue engineering, Biomaterials 30 (2009) 4996–5003.

[4] R. Kroeze, M. Helder, L. Govaert, T. Smit, Biodegradable polymers in bone tissue engineering, Materials 2 (2009) 833–856.
[5] C.M. Alves, Y. Yang, D. Marton, D.L. Carnes, J.L. Ong, V.L. Sylvia, D.D. Dean, R.L. Reis, C.M. Agrawal, Plasma surface modification of poly(D,L-lactic acid) as a tool to enhance protein adsorption and the attachment of different cell types, J. Biomed. Mater. Res. B: Appl. Biomater. 87B (2008) 59–66.
[6] J.M. Goddard, J.H. Hotchkiss, Polymer surface modification for the attachment of bioactive compounds, Prog. Polym. Sci. 32 (2007) 698–725.
[7] B.D. Ratner, A.S. Hoffman, F.J. Schoen, J.E. Lemons, Biomaterials Science Introduction to Materials in Medicine, 2nd Ed., Elsevier Academic Press, New York, 2004.
[8] Y. Wan, W. Chen, J. Yang, J. Bei, S. Wang, Biodegradable poly(L-lactide)-poly(ethylene glycol) multiblock copolymer: synthesis and evaluation of cell affinity, Biomaterials 24 (2003) 2195–2203.
[9] R. Morent, N. De Geyter, T. Desmet, P. Dubruel, C. Leys, Plasma surface modification of biodegradable polymers: a review, Plasma Process. Polym. 8 (2011) 171–190.
[10] M.T. Khorasani, H. Mirzadeh, S. Irani, Plasma surface modification of poly (L-lactic acid) and poly (lactic-co-glycolic acid) films for improvement of nerve cells adhesion, Radiat. Phys. Chem. 77 (2008) 280–287.
[11] M.C. Kim, T. Masuoka, Degradation properties of PLA and PHBV films treated with CO_2-plasma, React. Funct. Polym. 69 (2009) 287–292.
[12] J. Yang, J. Bei, S. Wang, Enhanced cell affinity of poly (D,L-lactide) by combining plasma treatment with collagen anchorage, Biomaterials 23 (2002) 2607–2614.
[13] Z. Guowei, G. Junping, G. Qiang, C. Yashao, Surface modification of biodegradable poly(D,L -lactic acid) by nitrogen and nitrogen/hydrogen plasma for improving surface hydrophilicity, Plasma Sci. Technol. 13 (2011) 230–234.
[14] T. Jacobs, R. Morent, N. Geyter, P. Dubruel, C. Leys, Plasma surface modification of biomedical polymers: influence on cell–material interaction, Plasma Chem. Plasma Process. 32 (2012) 1039–1073.
[15] Y. Jiao, J. Xu, C. Zhou, Effect of ammonia plasma treatment on the properties and cytocompatibility of a poly(L-lactic acid) film surface, J. Biomater. Sci. Polym. E. 23 (2012) 763–777.
[16] J. Yang, G. Shi, J. Bei, S. Wang, Y. Cao, Q. Shang, G. Yang, W. Wang, Fabrication and surface modification of macroporous poly(L-lactic acid) and poly(L-lactic-co-glycolic acid) (70/30) cell scaffolds for human skin fibroblast cell culture, J. Biomed. Mater. Res. 62 (2002) 438–446.
[17] T.P. Kunzler, C. Huwiler, T. Drobek, J. Vörös, N.D. Spencer, Systematic study of osteoblast response to nanotopography by means of nanoparticle-density gradients, Biomaterials 28 (2007) 5000–5006.
[18] P. Ying, Y. Yu, G. Jin, Z. Tao, Competitive protein adsorption studied with atomic force microscopy and imaging ellipsometry, Colloid. Surface. B 32 (2003) 1–10.
[19] H. Noh, E.A. Vogler, Volumetric interpretation of protein adsorption: competition from mixtures and the Vroman effect, Biomaterials 28 (2007) 405–422.
[20] D. Boonyawan, S. Sarapirom, S. Tunma, C. Chaiwong, P. Rachtanapun, R. Auras, Characterization and antimicrobial properties of fluorine-rich carbon films deposited on poly(lactic acid), Surf. Coat. Technol. 205 (Suppl. 2) (2011) S552–S557.
[21] A. Rudawska, E. Jacniacka, Analysis for determining surface free energy uncertainty by the Owen–Wendt method, Int. J. Adhes. Adhes. 29 (2009) 451–457.
[22] M. Żenkiewicz, Methods for the calculation of surface free energy of solids, J. Achievements Mater. Manuf. Eng. 24 (2007) 137–145.
[23] E.R. Fisher, A review of plasma–surface interactions during processing of polymeric materials measured using the IRIS technique, Plasma Proc. Polym. 1 (2004) 13–27.
[24] A. Fateev, F. Leipold, Y. Kusano, B. Stenum, E. Tsakadze, H. Bindslev, Plasma chemistry in an atmospheric pressure Ar/NH_3 dielectric barrier discharge, Plasma Proc. Polym. 2 (2005) 193–200.
[25] L. Bacakova, E. Filova, M. Parizek, T. Ruml, V. Svorcik, Modulation of cell adhesion, proliferation and differentiation on materials designed for body implants, Biotechnol. Adv. 29 (2011) 739–767.
[26] D. Luensmann, L. Jones, Albumin adsorption to contact lens materials: a review, Contact Lens and Anterior Eye 31 (2008) 179–187.
[27] C. González-García, S.R. Sousa, D. Moratal, P. Rico, M. Salmerón-Sánchez, Effect of nanoscale topography on fibronectin adsorption, focal adhesion size and matrix organisation, Colloid. Surface. B 77 (2010) 181–190.
[28] H.A. Mukhtar, A.B. John, L. James Mc, W. Ahmed, Study of human serum albumin adsorption and conformational change on DLC and silicon doped DLC using XPS and FTIR spectroscopy, J. Biomater. Nanobiotechnol. 4 (2013) 194–203.
[29] Z.X. Xu, T. Li, Z.M. Zhong, D.S. Zha, S.H. Wu, F.Q. Liu, W.D. Xiao, X.R. Jiang, X.X. Zhang, J.T. Chen, Amide-linkage formed between ammonia plasma treated poly(D,L-lactide acid) scaffolds and bio-peptides: enhancement of cell adhesion and osteogenic differentiation in vitro, Biopolymers 95 (2011) 682–694.
[30] A. Tache, S. Cotrone, S.-C. Litescu, N. Cioffi, L. Torsi, L. Sabbatini, G.L. Radu, Spectrochemical characterization of thin layers of lipoprotein self-assembled films on solid supports under oxidation process, Anal. Lett. 44 (2011) 747–760.
[31] S.R. Sousa, P. Moradas-Ferreira, B. Saramago, L. Viseu Melo, M.A. Barbosa, Human serum albumin adsorption on TiO_2 from single protein solutions and from plasma, Langmuir 20 (2004) 9745–9754.
[32] M. Bryjak, I. Gancarz, G. Poźniak, W. Tylus, Modification of polysulfone membranes 4. Ammonia plasma treatment, Eur. Polym. J. 38 (2002) 717–726.
[33] M.M. Browne, G.V. Lubarsky, M.R. Davidson, R.H. Bradley, Protein adsorption onto polystyrene surfaces studied by XPS and AFM, Surf. Sci. 553 (2004) 155–167.
[34] R.A. D'Sa, G.A. Burke, B.J. Meenan, Protein adhesion and cell response on atmospheric pressure dielectric barrier discharge-modified polymer surfaces, Acta Biomaterialia 6 (2010) 2609–2620.

CURRICULUM VITAE

Author's Name	Ms. Sureeporn Sarapirom
Date of Birth	20 September 1978
Place of Birth	Chiang Rai
Education	1994-1996 High school, Suanboonyopathum Lamphoon 1996-2000 B.Sc. (Physics) Chiang Mai University 2002-2004 M.B.A. Ramkhamhaeng University 2007-2009 M.S. (Applied Physics) Chiang Mai University 2010-2014 Ph.D. (Applied Physics) Chiang Mai University
Scholarship	2007-2014 The Thailand Center of Excellence in Physics
Publications	S. Sarapirom, Joon S. Lee, Su B. Jin, Doo H. Song, L.D. Yu ,Jeon G. Han, C. Chaiwong. "Wettability Effect of PECVD-SiO_x Films on Poly(lactic acid) Induced by Oxygen Plasma on Protein Adsorption and Cell Attachment" ScieTech 2013 IOP Publishing Journal of Physics: Conference Series, Vol.423, 2013, Page No. 012042. S. Sarapirom, L.D. Yu, D. Boonyawan, S. Intarasiri, C. Chaiwong. "Effect of Surface Modification of Poly (lactic acid) by Low-pressure Ammonia Plasma on Adsorption of Human Serum Albumin" Applied Surface Science, Vol.301, 2014, Page No. 45-50.
Training	2013 Institute for Plasma-Nano Materials, Center of Advanced Plasma Surface Technology, Sungkyunkwan University, Korea.
Presentations	S. Sarapirom, T. Tapala, T. Bunfong, D. Boonyawan, C. Chaiwong. "Synthesis of Carbon films with Various Fluorine Concentrations on Poly (lactic acid)" 9th Eco-Energy and Materials Science and Engineering Symposium (EMSES), Chiang Rai, Thailand. 25-28 May 2011. S. Sarapirom, W. Wongkham, D. Boonyawan, C. Chaiwong. "Adsorption of Focal Adhesion kinase on Ammonia Plasma Modified Poly (lactic acid)" Advanced Plasma Technology for Green Energy

and Biomedical Applications (APT 2011), Chiang Mai, Thailand. 11-12 Aug 2011.

S. Sarapirom, D. Boonyawan, W. Wongkham, L.D. Yu ,C. Chaiwong. "Surface Functionalization of Poly (lactic acid) Using Ammonia Plasma for Reducing Adsorption of Human Serum Albumin and Enhancing Cell Attachment" Taiwan Association for coatings and thin films technology (TACT 2011), Kenting, Taiwan. 20-23 Nov 2011.

S. Sarapirom, Joon S. Lee, Su B. Jin, Doo H. Song, L.D. Yu ,Jeon G. Han, C. Chaiwong. "Oxygen Plasma treatments of Silicon Oxide Films on Poly (lactic acid) to Control Protein Adsorption" Advanced Plasma Technology for Green Energy and Biomedical Applications (APT 2012), Chiang Mai, Thailand. 22-23 Aug 2012.

S. Sarapirom, Joon S. Lee, Su B. Jin, Doo H. Song, L.D. Yu ,Jeon G. Han, C. Chaiwong. "Wettability Effect of PECVD-SiO_x Films on Poly (lactic acid) Induced by Oxygen Plasma on Protein Adsorption and Cell Attachment" International Conference on Science & Engineering in Mathematics, Chemistry and Physics 2013 (ScieTech 2013), Jakarta, Indonesia. 24-25 Jan 2013.

S. Sarapirom, D. Boonyawan, L.D. Yu, S. Intarasiri, C. Chaiwong "Surface Functionalization of Poly (lactic acid) Using Ammonia Plasma for Reducing Adsorption of Human Serum Albumin" 18th International Conference on Surface Modification of Materials by Ion Beams (SMMIB 2013), Izmir, Turkey. 15-20 Sep 2013.